Available online at www.sciencedirect.com
SCIENCE DIRECT®
Remote Sensing of Environment 103 (2006) 474–487
Remote Sensing of Environment
www.elsevier.com/locate/rse

Improved land surface emissivities over agricultural areas using ASTER NDVI

Juan C. Jiménez-Muñoz [a], José A. Sobrino [a,*], Alan Gillespie [b], Donald Sabol [b], William T. Gustafson [b]

[a] Global Change Unit – Department of Thermodynamics – Faculty of Physics, University of Valencia, Dr Moliner 50-46100 Burjassot, Spain
[b] W. M. Keck Remote Sensing Laboratory – Department of Earth and Space Sciences, University of Washington, Seattle, Washington 98195–1310, USA

Received 6 May 2005; received in revised form 19 April 2006; accepted 22 April 2006

Abstract

Land surface emissivity retrieval over agricultural regions is important for energy balance estimations, land cover assessment and other related environmental studies. The Advanced Spaceborne Thermal Emission and Reflection Radiometer (ASTER) produces images of sufficient spatial resolution (from 15 m to 90 m) to be of use in agricultural studies, in which fields of crops are too small to be well-resolved by low resolution sensors. The ASTER project generates land surface emissivity images as a Standard Product (AST05) using the Temperature/Emissivity Separation (TES) algorithm. However, the TES algorithm is prone to scaling errors in estimating emissivities for surfaces with low spectral contrast if the atmospheric correction is inaccurate. This paper shows a comparison between the land surface emissivity estimated with the TES algorithm and from a simple approach using the Normalized Difference Vegetation Index (NDVI) for five ASTER images (28 June 2000, 15 August 2000, 31 August 2000, 28 April 2001 and 02 August 2001) of the agricultural area of Barrax (Albacete, Spain). The results indicate that differences are <1% for ASTER band 13 (10.7 μm) and <1.5% for band 14 (11.3 μm), but >2% for bands 10 (8.3 μm), 11 (8.6 μm) and 12 (9.1 μm). The emissivities for the five ASTER bands were tested against in situ measurements carried out with the CIMEL CE 312-2 field radiometer, the NDVI method giving root mean square errors (RMSE) <0.005 over vegetated areas and RMSE <0.015 over bare soil, and the TES algorithm giving RMSE ~0.01 for vegetated areas but RMSE >0.03 over bare soil. The errors and inconsistencies for ASTER bands 13 and 14 are within those anticipated for TES, but the greater errors for bands 10–12 suggest the presence of problems related to atmospheric compensation and model assumptions about soil spectra. The NDVI method uses visible/near-infrared data co-acquired with the thermal images to estimate vegetation cover and, hence, provides an independent constraint on emissivity. The success of this approach suggests that it may be useful for daytime images of agricultural or other heavily vegetated areas, in which the TES algorithm has occasional failures.

Keywords: Temperature; Emissivity; NDVI; TES; ASTER

1. Introduction

Land surface emissivity is a measure of the efficiency with which surfaces convert kinetic into radiant energy. Hemispheric emissivity varies with surface composition, including moisture, roughness, and particle size. Remotely determined emissivities also vary with observation conditions, wavelength, pixel resolution and observation angle. Emissivities may be diagnostic of composition, especially for the silicate minerals that make up much of the land surface (e.g., Lyon, 1965). Surface emissivities are thus important for studies of soil development and erosion and for estimating amounts and changes in sparse vegetation cover for which the substrate is visible, in addition to bedrock mapping and resource exploration.

Emissivity (ε) is a proportionality factor that scales blackbody radiance (Planck's law) to predict emitted radiance. Thus, ε must be known in order to estimate land surface temperature (T) accurately; this is important for global-change studies, estimation of radiation budgets, heat-balance studies and control for climate models.

* Corresponding author.
E-mail address: sobrino@uv.es (J.A. Sobrino).

0034-4257/$ - see front matter © 2006 Elsevier Inc. All rights reserved.
doi:10.1016/j.rse.2006.04.012

Even under ideal conditions in which a land surface element represented by a pixel is homogeneous and isotropic, estimating ε from the measured radiance is underdetermined. This is because, for every measured radiance, there is the unknown ε, plus *T*. Therefore, for most real surfaces the number of unknowns is $\geq n+1$, where *n* is the number of spectral channels or bands.

Because of the indeterminacy in solving for *T* and ε, a number of methods have been explored in order to retrieve land surface emissivity from satellite data (e.g., Becker & Li, 1990, 1995; Gillespie et al., 1998; Goïta & Royer, 1997; Kahle et al., 1980; Kealy & Hook, 1993; Sobrino & Raissouni, 2000; Watson, 1992). A summary of land surface temperature and emissivity methods can be found in Sobrino et al. (2002a) and Dash et al. (2002).

This paper deals with the problem of the land surface emissivity retrieval over agricultural areas, which mostly include surfaces with low spectral contrast. For this purpose, the NASA's Advanced Spaceborne Thermal Emission and Reflection Radiometer (ASTER) has been used. The ASTER imager, on board the Terra satellite (launched 19 December 1999), contains a five-channel thermal infrared (TIR: 8–12 μm) scanner that produces images of sufficient field of view (60 km), spatial resolution (90 m) and radiometric resolution ($NE\Delta T_{300K} < 0.3$ K) to be of use in agricultural studies, in which fields of crops are too small to be well-resolved by MODIS, AVHRR or AATSR. The ASTER project generates Standard Products from these images (*T* — AST08; ε — AST05) that are designed to work over rock surfaces as well as vegetation and water, and during the night as well as the day. ASTER also collects three 15 m visible/near-infrared (VNIR) channels suitable for calculating NDVI (Normalized Difference Vegetation Index).

In the present paper, we compare the performance of the emissivity retrieval from NDVI values (referred as the NDVI method) to the Temperature/Emissivity Separation (TES) algorithm for daytime images of the Barrax site. In the TES algorithm (Gillespie et al., 1998), surface emissivities are calculated from TIR image data alone; in the NDVI method, surface emissivities are predicted from visible and near infrared bands. Use of the NDVI method for agricultural studies is attractive because TES is prone to scaling errors in estimating ε for vegetation if the atmospheric correction is inaccurate, as will be explained in Section 2.4, whereas the NDVI method identifies vegetated areas for which ε is known a-priori. Because of the scaling problem, the TES algorithm that created the Standard Products cannot be optimized for agricultural applications.

The paper is organized as follows: Section 2 presents the study area, the satellite and field data, the ASTER data processing and a description of the TES and NDVI methods, whereas Section 3 shows the results obtained with both methods over different plots and the test using field measurements collected in the study area in the framework of different field campaigns. Use of VNIR and TIR data to discriminate different crops is also discussed in Section 3. Finally, Section 4 includes a summary and the main conclusions drawn from this study.

2. Methods

2.1. Study area

The study area is located at Barrax, in the La Mancha region of Spain. It is on a plateau ~700 m above sea level, with elevation differences <2 m over the whole test area. The 10,000 ha Barrax site (39°3′ N, 2°6′ W) is in the western part of the province of Albacete, 28 km NE from the capital town of the same name. The area was selected for its flat terrain, minimising the complications introduced by variable lighting geometry, and the presence of large, uniform land-use units suitable for validating the moderate-resolution satellite image products. The Barrax test site has previously been used for remote-sensing experiments such as the EFEDA (European International Project on Climatic and Hydrological Interactions between Vegetation, Atmosphere and Land Surface, Field Experiment in Desertification Threatened Areas) experiment in 1991, the Digital Airborne Imaging Spectrometer Experiment (DAISEX) in 1998, 1999 and 2000, the SPECTRA Barrax Campaign (SPARC) in 2003 and 2004, and the Sentinel-2 Fluorescence Experiment (SEN2FLEX) in 2005.

The climate at Barrax is of Mediterranean type, with heaviest rainfalls in spring and autumn and lowest in summer; it presents a high level of continentality, with quite sudden changes from cold months to warm months and high thermal oscillations in all seasons between the maximum and minimum daily temperatures. The rainfall statistics show that the mean annual rainfall is little more than 400 mm in most of the area, making La Mancha one of the driest regions in Europe. Precipitation is seasonal, with a minimum in summer (June–August) and a high year-to-year variability.

The soils of the area have been poorly developed. In terms of soil taxonomy they are Inceptisols. They are very finely textured and have a high degree of compactness under drying conditions. All soils show a calcic hard-pan layer at approximately >40 cm below the surface. The main limitation offered by the soils with regard to their productive capacity is their small depth, due to the presence of the petrocalcic horizon with large amounts of limestone. The stoniness is excessive in many cases due to the presence of remains of petrocalcic horizon on the surface. About 65% of cultivated lands at Barrax are dryland (67% winter cereals; 33% fallow) and 35% irrigated land (75% corn; 15% barley/sunflower; 5% alfalfa; 5% onions and vegetables). The University of Castilla-La Mancha, through the "Escuela Técnica Superior de Ingenieros Agrónomos," operates three agro-meteorological stations in the study area. More details about the test site are presented in Moreno et al. (2001).

2.2. Satellite and field data

Five daytime ASTER images acquired over the Barrax site for two consecutive years were used: 28 June, 15 August and 31 August in 2000; and 28 April and 2 August in 2001. Overpass time was close to 11:20 GMT. ASTER provides images in Visible/Near-Infrared (VNIR) with a spatial resolution of 15 m, in Shortwave-Infrared (SWIR) with a spatial resolution of 30 m,

and in TIR with a spatial resolution of 90 m (Abrams, 2000). We used VNIR bands 2 (0.63–0.69 μm) and 3 (0.76–0.86 μm) to predict ε with the NDVI approach, whereas TIR bands 10 (8.125–8.475 μm), 11 (8.475–8.825 μm), 12 (8.925–9.275 μm), 13 (10.25–10.95 μm) and 14 (10.95–11.65 μm) are used to estimate ε with TES.

Field measurements were carried out over the Barrax test site in the framework of the SPARC (2004) and SEN2FLEX (2005) campaigns. The TES method applied to ground-based measurements collected with the CIMEL CE 312-2 field TIR radiometer was used to obtain in situ ε measurements for crops and soils. The CIMEL CE 312-2 has five spectral bands in coincidence with the ASTER TIR bands, and also one broad band (8–13 μm). It has a field of view (FOV) of 10° and a $NE\Delta T_{293K}$ of 0.008 K for the broad band and 0.050 K for the five spectral bands. An analysis of the TES as a simple method to retrieve surface emissivities from ground-based measurements is presented in Payan and Royer (2004). In order to test the emissivity spectra provided by the NDVI and TES methods over the different crops, the field measurements have been complemented with the laboratory spectra included in the ASTER spectral library (ASTERlib) (available on-line at http://speclib.jpl.nasa.gov). In addition, one sample of soil was collected in the field and sent to the Jet Propulsion Laboratory (JPL). The emissivity spectrum of the soil was measured in the JPL with the Nicolet spectrometer (http://speclib.jpl.nasa.gov/documents/jpl_desc.htm).

Fig. 1 shows the study area and the plots where emissivity spectra have been extracted from the image. Three different plots have been considered during the study period: P1 was alfalfa and P2 was irrigated corn, whereas P3 was bare soil in 2000 and non-irrigated barley in 2001. In order to extract values from the mentioned images, boxes of 3×3 pixels at the TIR resolution (90 m) belonging to the different crops analyzed have been considered. These boxes selected have an approximate total size of 7 ha and will provide values statistically reliable. The standard deviation value of the pixels included in the different boxes will provide information about the surface homogeneity in terms of emissivity. Because the ASTER VNIR bands have a resolution of 15 m, the boxes of 3×3 pixels at the TIR resolution were overlapped to the VNIR images using the geographic coordinates included in the ASTER images (geometric correction), leading to boxes of 18×18 pixels at the VNIR scale. Problems related with the up-scaling problem are not discussed in this paper, but these problems are expected to be negligible over agricultural areas with low variability on emissivity values.

2.3. ASTER data processing

ASTER provides the user community with Standard Data Products processed to different Levels. Level-1 products contain the radiance at sensor, whereas Level-2 products have been compensated for atmospheric absorption and emission (land-leaving radiance), and include surface T and ε data. In the present study we used two Level-2 Standard Products: at-surface VNIR reflectivities (AST-07) to predict ε with the NDVI

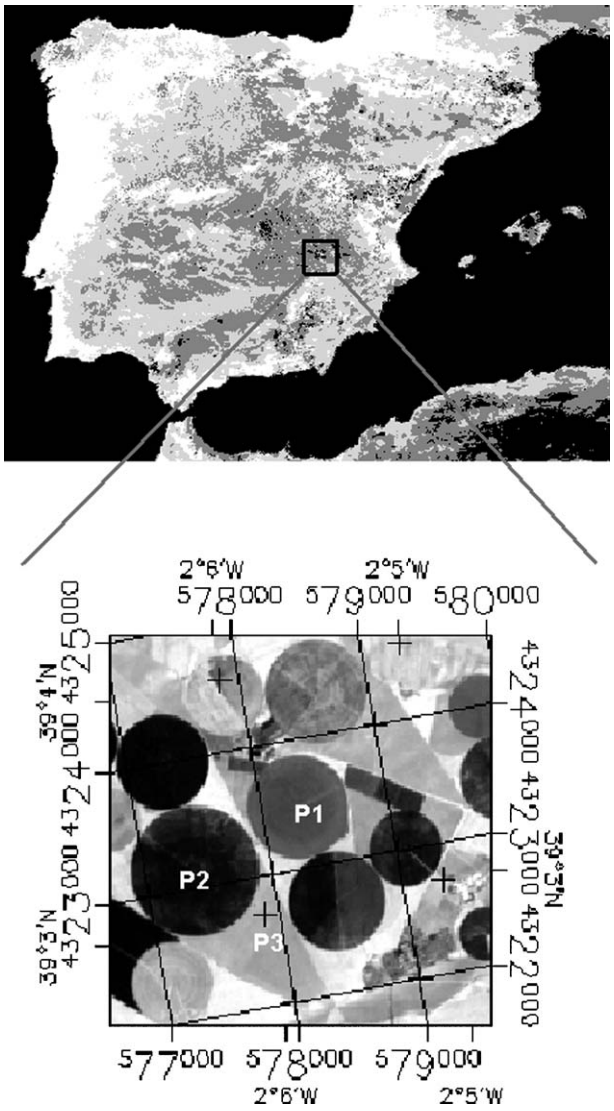

Fig. 1. The study area of Barrax. Location over the Iberian Peninsula and index map using ASTER band 2 (pixel size: 15 m). The ASTER image was acquired on 28 June 2000. The plots considered in the study are also shown: P1 = alfalfa, P2 = irrigated corn, P3 = bare soil in 2000 and P3 = non-irrigated barley in 2001.

method (Section 2.5), and TIR emissivities (AST-05) estimated with the TES method. Fig. 2 shows some examples of these products.

At-surface reflectivities are obtained from land-leaving radiances corrected for solar irradiance. Atmospheric correction for the VNIR data is based upon a look-up table (LUT) approach summarizing results from a Gauss–Seidel iteration radiative transfer code (Herman & Browing, 1965). The method has its basis in the reflectance-based, vicarious-calibration approach of Slater et al. (1987). The method currently assumes atmospheric scattering optical depths and aerosol parameters are known independently of ASTER data. Using these parameters and the LUT, piecewise-linear fits are determined that relate the at-sensor radiances to surface radiance and surface reflectance. The method has some constraints, and is only applicable for clear-sky conditions. Details can be found in Thome et al. (1999).

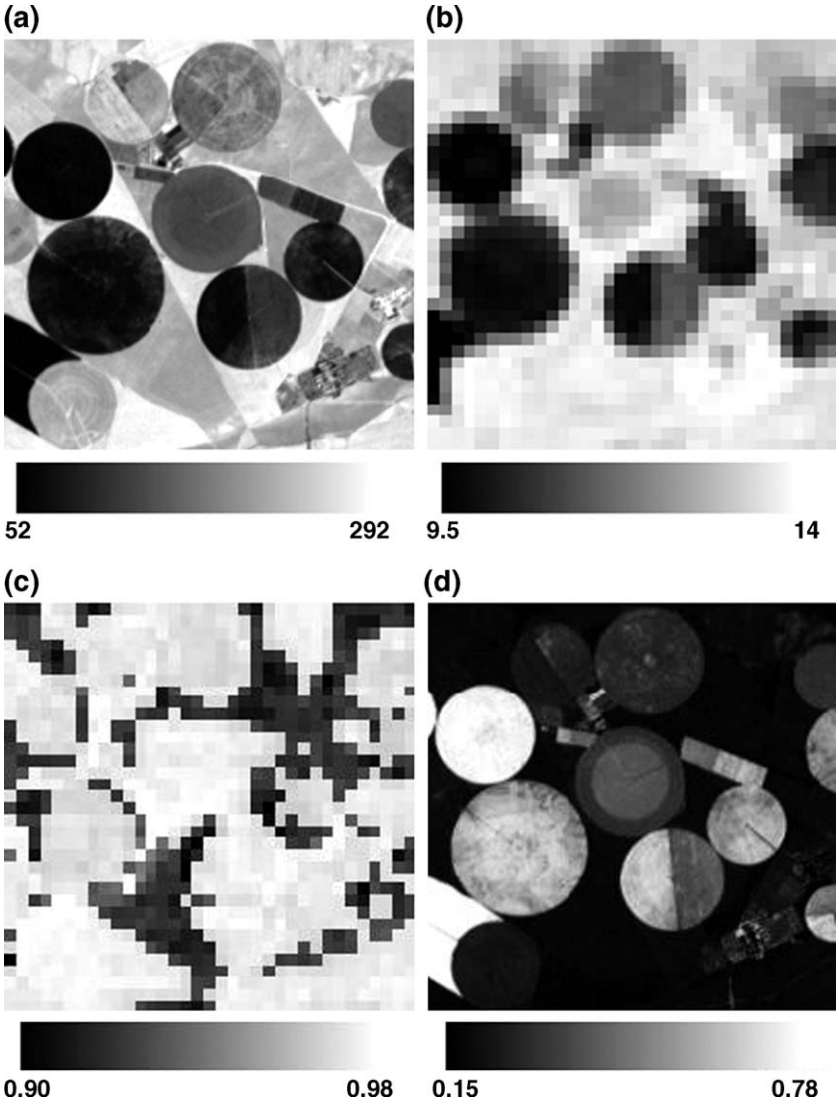

Fig. 2. ASTER Standard Data Products over Barrax for an image acquired on 28 June 2000: a) ASTER channel 2 VNIR land-leaving radiance (units in $Wm^{-2}\ sr^{-1}\ \mu m^{-1}$); b) ASTER channel 12 TIR land-leaving radiance (units in $Wm^{-2}\ sr^{-1}\ \mu m^{-1}$); c) ASTER channel 12 TIR emissivity; d) NDVI image calculated from ASTER bands 3 and 2.

TIR emissivities included in the Standard Product AST-05 are calculated by TES (Section 2.4) applied to land-leaving TIR radiances. The method used for atmospheric correction of the ASTER thermal data is a clear-sky method not applicable close to clouds. It is based on the radiative transfer equation and uses the MODTRAN radiative transfer code, Version 3.5 (Abreu & Anderson, 1996). In order to perform the atmospheric correction, the method requires all the necessary atmospheric parameters, including temperature, water vapour, ozone, and aerosol profiles at the time and location of the measurements to be corrected. NASA's plan called for these characteristics to be determined from other instruments aboard Terra. However, currently NCEP GDAS (National Centers for Environmental Prediction Global Data Assimilation System) atmospheric profiles on 1-degree centres updated every 6 h from radiosonde data are used instead, together with a 1-km DEM. More details are presented in Palluconi et al. (1999).

2.4. Temperature and Emissivity Separation Method: TES

The TES (Temperature and Emissivity Separation) method estimates land surface emissivity ε_i and temperature T from ASTER land-leaving thermal data and down-welling atmospheric irradiances (Gillespie et al., 1998). It is based on the radiative transfer equation applied to thermal data, in which the land-leaving radiance (L_i^{LLR}) for band i is given by

$$L_i^{\mathrm{LLR}} = \varepsilon_i B_i(T_s) + \pi^{-1}(1-\varepsilon_i)L_i^{\mathrm{atm}\downarrow} \quad (1)$$

where B_i is Planck's function, T_s the land surface temperature and $L_i^{\mathrm{atm}\downarrow}$ the down-welling atmospheric irradiance.

In order to completely determine Eq. (1) from the five ASTER bands (six unknowns) it is necessary to supply one independent measurement. ASTER uses a semi-empirical relation determined from laboratory spectra, between the minimum

emissivity and spectral contrast (maximum–minimum difference, MMD).

Taking into account that L_i^{LLR} and $L_i^{\mathrm{atm}\downarrow}$ are the input data, from an initial value of emissivity it is possible to obtain a first value for land surface temperature. In fact, five different values will be obtained for T_s using Eq. (1) by inversion of Planck's law for each ASTER thermal band. The final value for T_s is chosen as the maximum value between the five different values. Then, T_s can be introduced again in Eq. (1) and obtain the emissivity values for ASTER thermal bands. This methodology can be repeated again in order to obtain another value for T_s and other emissivity values. The described iterative procedure is called as NEM (Normalized Emissivity Method) module, and constitutes itself a method for retrieving surface emissivities and temperature (Gillespie, 1985). In order to obtain more accurate emissivity values, another two modules are applied: the RATIO and the MMD (Maximum–Minimum Difference) modules. The RATIO module obtains relative emissivities (β_i) by rationing the NEM emissivities to their average value, whereas in the MMD module final emissivity values are obtained according to the following expression:

$$\varepsilon_i = \beta_i \left(\frac{\varepsilon_{\min}}{\min(\beta_i)} \right) \tag{2}$$

where $\varepsilon_{\min}$ is the minimum emissivity obtained from the following empirical relationship:

$$\varepsilon_{\min} = 0.994 - 0.687\ \mathrm{MMD}^{0.737} \tag{3}$$

with MMD the spectral contrast calculated as

$$\mathrm{MMD} = \max(\beta_i) - \min(\beta_i) \tag{4}$$

The TES method is capable of recovering surface emissivities within about 0.015 and surface temperatures within about 1.5 K. A detailed description of the algorithm is given in Gillespie et al. (1998).

For surfaces with low spectral contrast (MMD<0.03), the relationship between $\varepsilon_{\min}$ and MMD given in Eq. (3) does not provide satisfactory results, and the TES algorithm sets $\varepsilon_{\min}$ to 0.983, a value appropriate for water and vegetation canopies (Gillespie et al., 1998). The MMD thershold improves computations of temperatures over targets with low MMD, but necessarily leads to problems where targets emissivites lie close to the threshold value (~0.03). The problems related to the TES thresholding are referred as the 'scaling errors', which necessarily correspond to a jump in the scaling value which creates artifactual contouring or step discontinuities in the image where there is a transition from vegetation to soil. Persistent calibration problems led to increasing the problem with the MMD threshold, which increased the severity of the "jump." Inaccuracies in atmospheric compensation are amplified, especially by the iterative correction for reflected downwelling sky irradiance, which jointly with the calibration problems tend to add scatter to the spectrum falsely increasing the spectral contrast. The atmospheric issues have led to high errors in band 10 emissivities especially, well above (~0.08) the nominal accuracy of ~0.015.

This serious, occasional failure is thought to occur at high atmospheric temperatures, low elevations, and total column water >1.7 g cm^{-2}. Thorough documentation of these matters is in preparation by A. R. Gillespie. It is a strong motivation for exploring new techniques for agricultural and other uses.

2.5. Land surface emissivity from NDVI values

Because problems in TES arise in differently scaling high- and low-MMD emissivity spectra, it makes sense to exploit the co-acquired VNIR data of ASTER to estimate vegetation cover and surface emissivity, independent of the TIR data.

Different approaches have been used to predict land surface emissivity from NDVI values (e.g., Sobrino & Raissouni, 2000; Valor & Caselles, 1996; Van de Griend & Owe, 1993). Most of them are based on the following simplified equation for homogeneous and flat surfaces:

$$\varepsilon_i = \varepsilon_{\mathrm{vi}} P_{\mathrm{V}} + \varepsilon_{\mathrm{si}}(1 - P_{\mathrm{V}}) \tag{5}$$

where $\varepsilon_{\mathrm{vi}}$ and $\varepsilon_{\mathrm{si}}$ are band emissivity values for vegetation and bare soil, respectively, and P_{V} is the proportion of vegetation or fractional vegetation cover. A cavity term should be added to Eq. (5) over rough surfaces, which could be calculated from geometrical models (Sobrino et al., 1990). The main constraint in using geometrical models is that a priori knowledge of some geometrical parameters as height, width and separation of the crops is needed. According to Sobrino et al. (1990), the cavity effect for a mixed area and near nadir view is given by $(1-\varepsilon_s)\varepsilon_v F'(1-P_V)$, where F' is a geometrical factor ranging between 0 and 1. Therefore, in areas with high soil emissivities the cavity term is not important. For example, assuming a mean value $F'=0.5$, a mean vegetation cover $P_V=0.5$, and $\varepsilon_v=0.99$ and $\varepsilon_s=0.96$, the cavity effect is less than 0.01. For these reasons, the cavity effect has been neglected when Eq. (5) is applied to the Barrax area. Cavity effects have been only accounted by adding a slightly increase on the vegetation emissivity ($\varepsilon_v=0.985+0.005$), according to Sobrino and Raissouni (2000).

P_{V} can be obtained from NDVI values according to (Carlson & Ripley, 1997):

$$P_{\mathrm{V}} = \left(\frac{\mathrm{NDVI} - \mathrm{NDVI_s}}{\mathrm{NDVI_v} - \mathrm{NDVI_s}} \right)^2 \tag{6}$$

where $\mathrm{NDVI_v}$ and $\mathrm{NDVI_s}$ are the NDVI values of full vegetation cover ($P_V=1$) and bare soil ($P_V=0$), respectively, which can be obtained from the NDVI histogram. Eq. (6) provides acceptable results over agricultural areas, with an accuracy of around 15%, which is a value accurate enough to retrieve surface emissivities from Eq. (5) (Jiménez-Muñoz et al., submitted for publication). The NDVI values have been obtained using ASTER bands 2 (red) and 3 (near-infrared) extracted from the ASTER product AST-07 (surface reflectance). For those pixels with $\mathrm{NDVI}<\mathrm{NDVI_s}$ the proportion of vegetation has been set to zero, whereas for those pixels with $\mathrm{NDVI}>\mathrm{NDVI_v}$ it has been set to 1.

The critical issue in Eq. (5) is the selection of the soil emissivities. The ASTERlib includes 49 soil emissivity spectra classified in terms of soil taxonomy as Alfisol (9 samples),

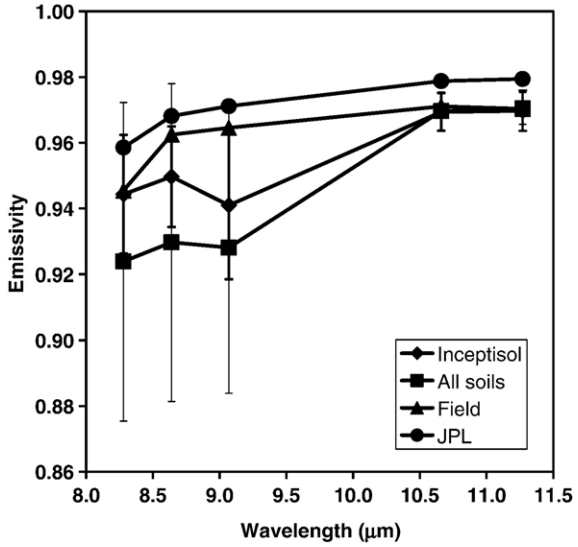

Fig. 3. Average emissivity spectra for different soil samples included in the ASTER spectral library (http://speclib.jpl.nasa.gov). 'Inceptisol' refers to the mean value for all the soil samples included in the ASTER library and classified as Inceptisol (7 samples). These values have been chosen a soil emissivities in the NDVI method. 'All soils' referes to the mean value for all the soil samples included in the ASTERlib (49 samples). Error bars refer to the standard deviation of the mean values. The emissivity spectrum obtained from field measurements (Field) and the one measured in the JPL are also given for comparison.

Aridisol (14 samples), Entisol (10 samples), Inceptisol (7 samples) and Mollisol (9 samples). Fig. 3 shows the mean soil emissivity spectrum for all the soil samples and also the mean spectrum only for the Inceptisol samples, which is the soil class of the Barrax area. Emissivity spectra measured in the field and in the Jet Propulsion Laboratory (JPL) are also graphed. The mean values for all the soil samples show high standard deviations (>0.04) in the 8–9.5 μm spectral range. Values measured in the field or laboratory should be the most accurate, but a priori knowledge of the site is required. For these reasons, a mean value for the Inceptisol class has been finally chosen in order to apply Eq. (5), despite that band 12 (9.1 μm) is expected to provide the worst results due to its high standard deviation (>0.02). Thus, surface emissivities can be estimated from NDVI for each ASTER thermal band according to the following expressions:

$$\varepsilon_{10} = 0.946 + 0.044\ P_V \quad (7a)$$

$$\varepsilon_{11} = 0.949 + 0.041\ P_V \quad (7b)$$

$$\varepsilon_{12} = 0.941 + 0.049\ P_V \quad (7c)$$

$$\varepsilon_{13} = 0.968 + 0.022\ P_V \quad (7d)$$

$$\varepsilon_{14} = 0.970 + 0.020\ P_V \quad (7e)$$

3. Results and discussion

In order to analyze the emissivity spectra obtained from TES and NDVI methods, four different cases have been considered according to different spectral signatures: fully vegetated areas (Section 3.1), bare soil (non-vegetated areas) (Section 3.2), mixed areas (Section 3.3) and senescent vegetation (Section 3.4). Fig. 4 shows the NDVI and P_V values for the plots considered in the study and described in Section 2.2. P_V has been calculated from Eq. (6), using the $NDVI_s$ and $NDVI_v$ values presented in Table 1. The alfalfa plots (P1) on 15-Aug-00, 31-Aug-00, 28-Apr-01 and 2-Aug-01, and the corn plots (P2) on 15-Aug-00 and 31-Aug-00 show P_V>90%, so they were considered as fully vegetated areas. The corn plot on 28-Apr-01 was not planted and the alfalfa plot on 28-Jun-00 was cut, so they are not shown in the results. Corn plots on 28-Jun-00 and 2-Aug-00 are not fully covered ($P_V \sim 65\%$), so they have

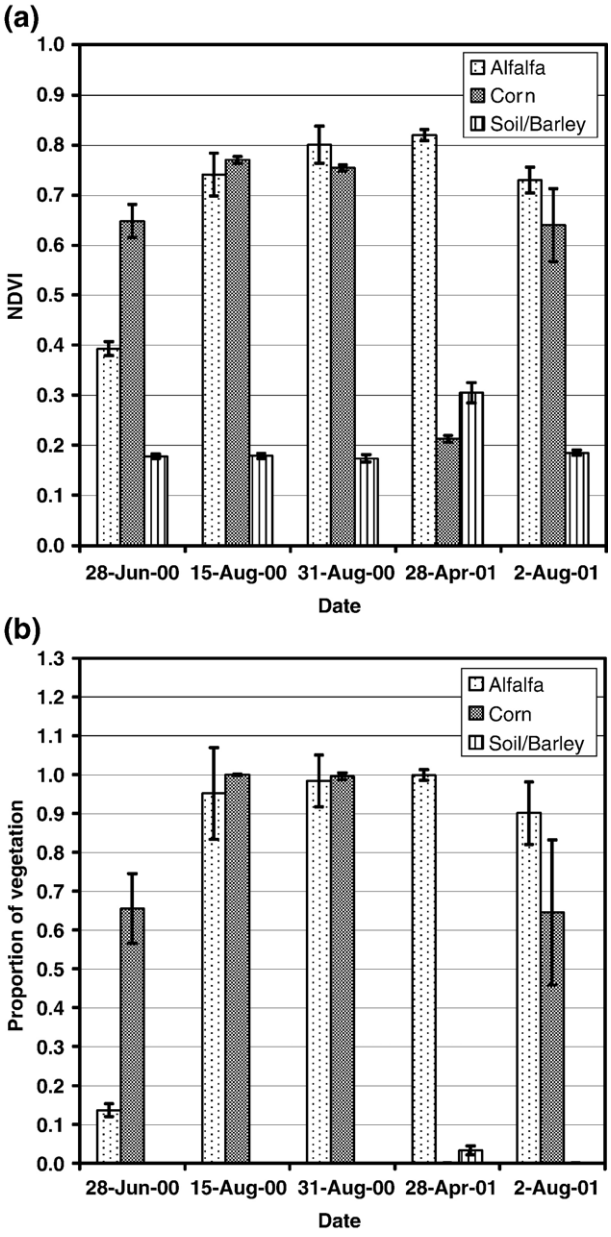

Fig. 4. Values of a) NDVI calculated from ASTER bands 3 and 2, and b) proportion of vegetation (P_V) estimated from Eq. (6), extracted from ASTER images acquired on different dates and for different plots. Standard deviation for the boxes of 18×18 pixels (at VNIR scale) is also plotted.

Table 1
NDVI values of bare soil ($NDVI_s$) and full vegetation cover ($NDVI_v$) used to estimate the proportion of vegetation from Eq. (6)

Date	$NDVI_s$	$NDVI_v$
28-Jun-2000	0.18	0.76
15-Aug-2000	0.18	0.75
31-Aug-2000	0.18	0.75
28-Apr-2001	0.20	0.79
2-Aug-2001	0.18	0.76

The values have been extracted from the NDVI histogram.

been considered as mixed areas. P3 was bare soil on 28-Jun-00, 15-Aug-00 and 31-Aug-00, and non-irrigated barley (senescent vegetation) on 28-Apr-01 and 2-Aug-01. The emissivity spectra obtained with NDVI and TES methods are first compared to laboratory spectra included in the ASTERlib in order to analyze the shape of the spectra, whereas in Section 3.5 the results are compared to field measurements in order to test the accuracy of the methods. Section 3.6 shows the NDVI and MMD values obtained with the two methods, and how to use them to distinguish between bare soil, green vegetation and senescent vegetation.

3.1. Fully vegetated areas

Fully vegetated areas are approximate blackbodies. The emissivity spectrum is nearly constant and near unity. Therefore, estimating the emissivity spectrum for these types of surface is less important than for surfaces of soils or rock. In fact, the NDVI approach assumes a constant value of 0.99 for these areas,

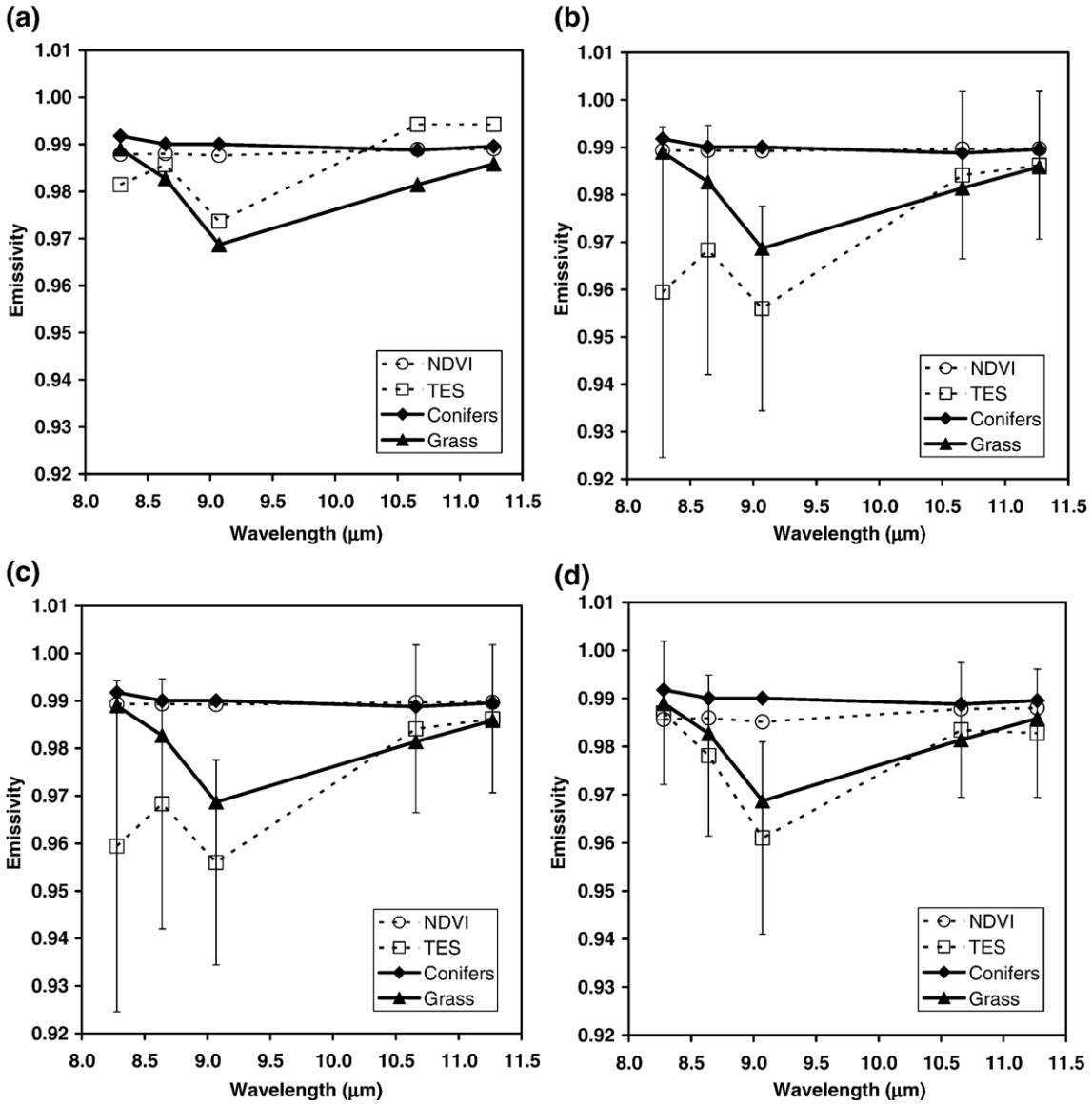

Fig. 5. Emissivity spectra obtained with the NDVI and TES methods for the alfalfa plot (fully vegetated area) and extracted from ASTER images acquired on a) 15 August 2000, b) 31 August 2000, c) 28 April 2001 and d) 2 August 2001. The conifer and grass emissivity spectra included in the ASTER spectral library are also shown for comparison. The error bars refer to the standard deviation of sampled 3 × 3 pixels at the TIR scale (90 m). Error bars for the NDVI method are not graphed because they are negligible (<0.005).

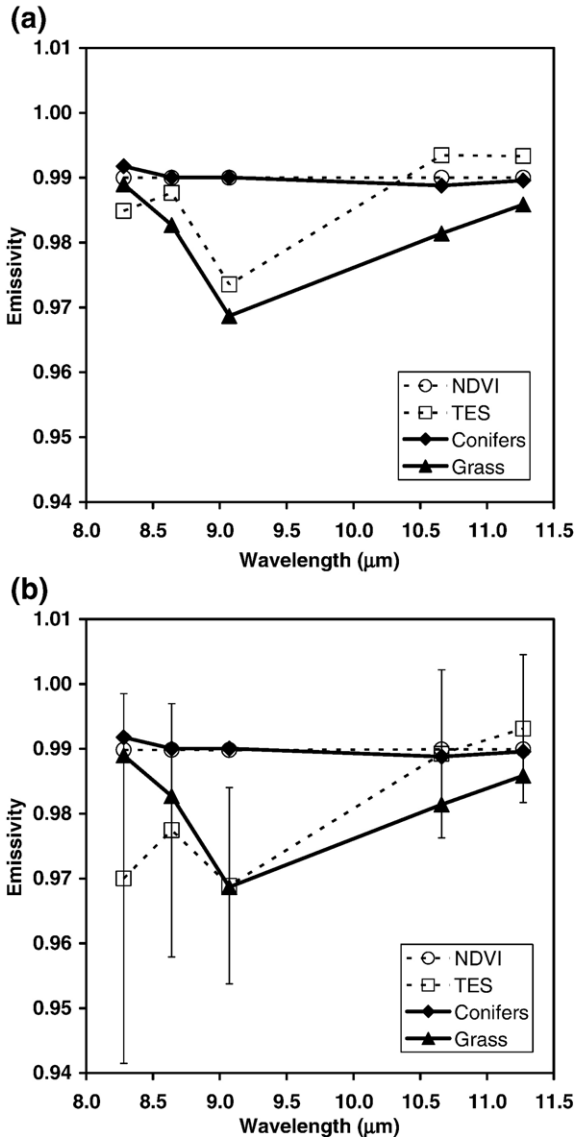

Fig. 6. Emissivity spectra obtained with the NDVI and TES methods for the corn plot (fully vegetated area) and extracted from ASTER images acquired on a) 15 August 2000 and b) 31 August 2000. The conifer and grass emissivity spectra included in the ASTER spectral library are also shown for comparison. The error bars refer to the standard deviation of sampled 3×3 pixels at the TIR scale (90 m). Error bars for the NDVI method are not graphed because they are negligible (<0.005).

whereas the TES algorithm assumes a fixed value for the minimum emissivity $\varepsilon_{min}=0.983$. Fig. 5 shows for the alfalfa plot (P1) the emissivity spectra obtained with the TES and NDVI methods and extracted from the different ASTER images. Laboratory conifer and grass vegetation spectra extracted from the ASTERlib are graphed for reference. In general, the NDVI method predicts emissivity spectra similar to the conifer spectrum, showing a high degree of homogeneity over the test areas. However, the TES method provides an emissivity spectrum similar to the grass one, although with higher standard deviation values than the NDVI method. Fig. 6 shows the emissivity spectra for the corn plot. Again, the emissivity spectra retrieved from the NDVI is similar to the conifers spectrum, whereas the spectra obtained with the TES is similar to the grass one, also with high standard deviation values. Extremely high standard deviation values (between 0.02 and 0.03) suggest that the TES method classified some pixels as low MMD and other pixels as high MMD, which show the problem related with the MMD threshold and the 'jump' commented in Section 2.4.

3.2. Bare soil

A fallow, bare-soil plot (P3 in 2000), which belongs to the Inceptisols in terms of soil taxonomy, was used to analyze the results obtained over non-vegetated areas. Fig. 7 shows the emissivity spectra obtained with the NDVI and TES method for bare soil. The spectrum obtained from laboratory measurements in the JPL is also shown. Both methods provide a similar shape for the spectrum, with the NDVI method providing slightly higher values than the TES method and also closer to the JPL spectrum. Despite that the soil spectrum should provide an increasing emissivity with increasing wavelength, a decrease is observed in band 12 (~9.1 μm) for the NDVI method and in bands 12 and 14 (~11.3 μm) for the TES method. The decrease observed in the NDVI method for band 12 is due to the high variability on the soil emissivities in this spectral region (see Fig. 3). The standard deviation values for the pixels included in the box selected over the image are zero for the NDVI method, which means that all the pixels were classified as bare soil ($NDVI<NDVI_s$), and lower than 0.01 for the TES method, which suggests that all the pixels were scaled as low spectral contrast (MMD) and the scaling problem did not occur in this particular case. Moreover, NDVI and TES methods provide similar results for bands 13 and 14, located in the spectral range 10–12 μm.

3.3. Mixed areas

Mixed areas are composed of bare soil and vegetation, so their emissivity spectra are expected to be formed by linear mixing for a percentage of bare soil and a complementary percentage of vegetation, depending on the proportion of vegetation (Eq. (5)). The emissivity spectra should be also elevated from laboratory values by the cavity effect, despite it has been neglected in Eq. (5) as has been commented in Section 2.5. The emissivity spectra obtained from the TES and NDVI methods are presented in Fig. 8 for corn with $P_V \sim 65\%$. The emissivity spectrum provided by the NDVI approach shows a similar shape than the soil spectrum (see Fig. 7), since the method assumes a constant contribution for the vegetation. Emissivity values are also closer to the vegetion ones than the values for bare soil, since P_V exceeds 50%. The standard deviation values are higher than in the previous cases, due to the high heterogeneity over mixed areas. The TES method provides a shape for the spectrum similar to the grass one (see Fig. 5) with high standard deviation values. In this case the high standard deviation values could be due to the high heterogeneity of mixed areas instead of the problems related with the MMD threshold, or may be to a combination of both effects.

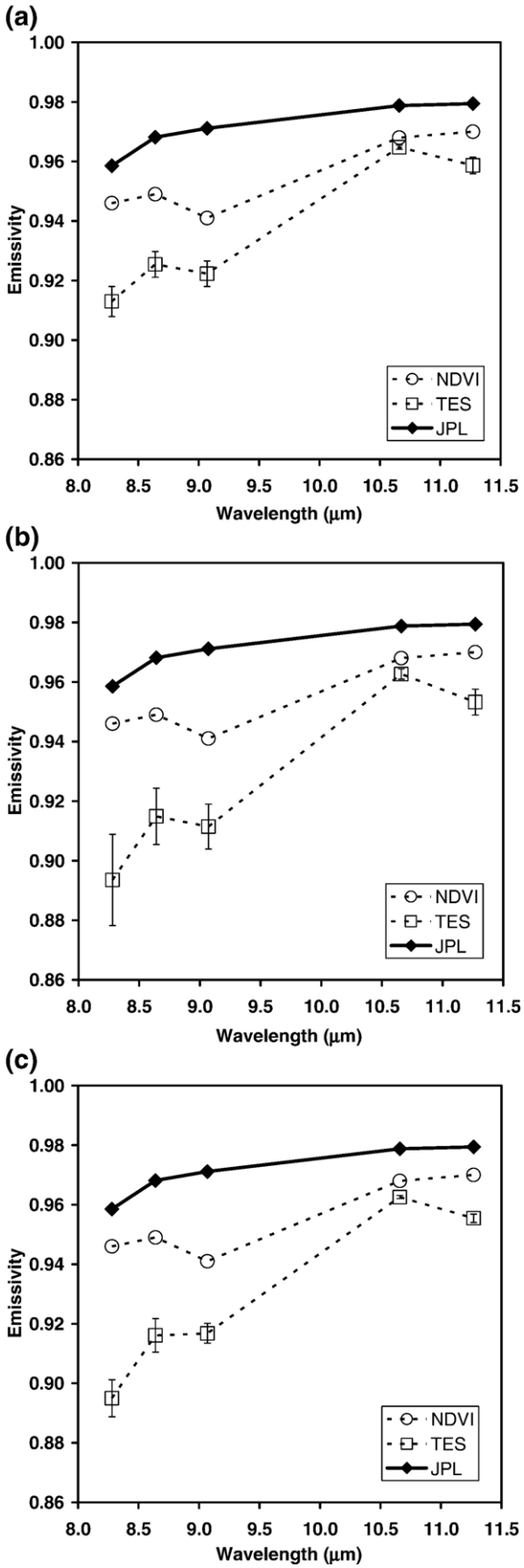

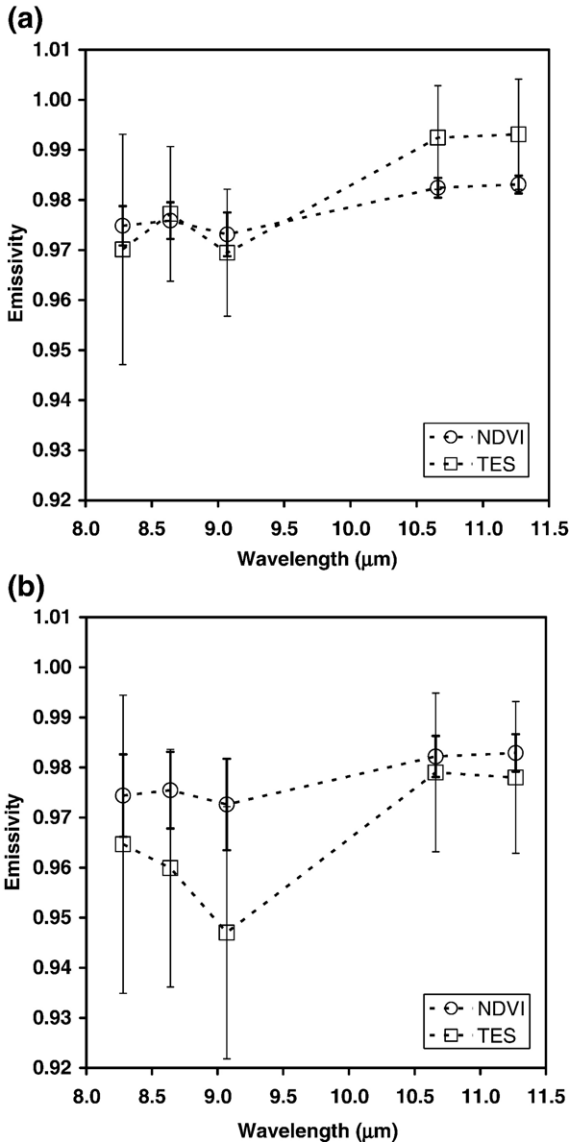

Fig. 8. Emissivity spectra obtained with the NDVI and TES methods for the corn plot (mixed area, $P_V \sim 65\%$) and extracted from ASTER images acquired on a) 28 June 2000 and b) 2 August 2001. The error bars refer to the standard deviation of sampled 3 × 3 pixels at the TIR scale (90 m) or 18 × 18 pixels at the VNIR scale (15 m).

3.4. Senescent vegetation

A non-irrigated barely plot (P3 in 2001) has been selected in order to analyze the results obtained over senescent vegetation. Fig. 9 shows the emissivity spectra obtained from NDVI and TES methods, and also the laboratory spectrum of the dry grass. The NDVI method classifies the pixels included in the non-irrigated barley plot as bare soil ($NDVI < NDVI_s$), so it provides the same emissivity spectrum as for bare soil (see Fig. 7). The

Fig. 7. Emissivity spectra obtained with the NDVI and TES methods for the bare soil plot and extracted from ASTER images acquired on a) 28 June 2000, b) 15 August 2000 and c) 31 August 2000. The emissivity spectrum measured in the JPL is also shown for comparison. The errors bars refer to the standard deviation of sampled 3 × 3 pixels at the TIR scale (90 m). Error bars for the NDVI method are not graphed because they are negligible (<0.005).

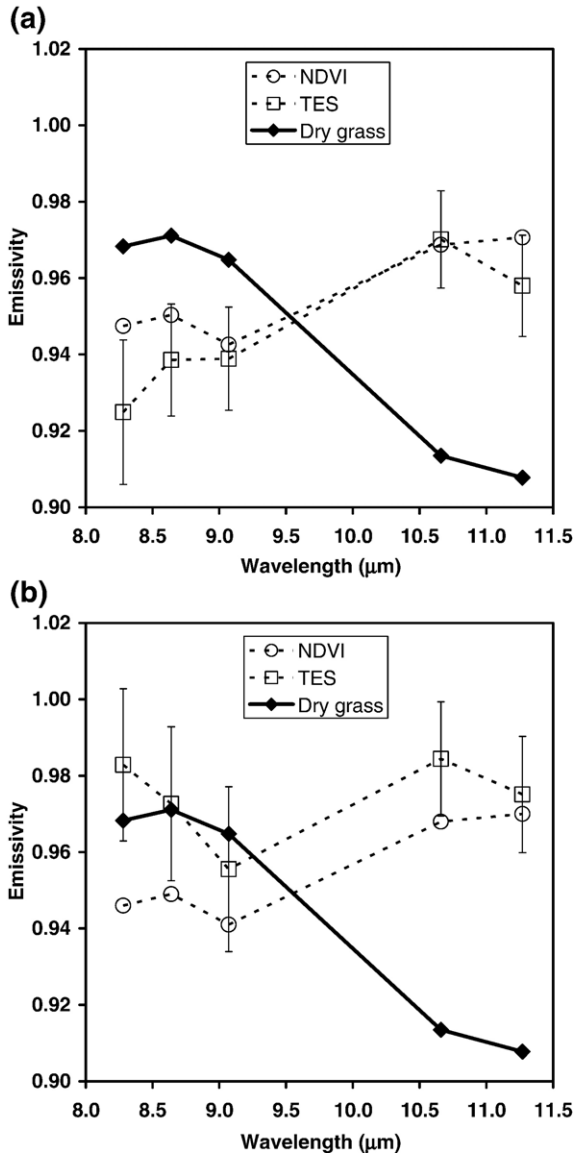

Fig. 9. Emissivity spectra obtained with the NDVI and TES methods for the non-irrigated barley plot and extracted from ASTER images acquired on a) 28 April 2001 and b) 2 August 2001. The dry grass emissivity spectrum included in the ASTER spectral library is also shown for comparison. The errors bars refer to the standard deviation of sampled 3 × 3 pixels at the TIR scale (90 m). Error bars for the NDVI method are not graphed because they are negligible (<0.005).

TES method also provides a typical soil spectrum for the barley plot on 28-Apr-01. However, the TES method provides a grass spectrum for the barley plot on 2-Aug-01. High standard deviation values have been also obtained. Neither of the methods follows the decrease on emissivity with increasing wavelength, as is shown by the dry grass spectrum, despite this could be due to a cavity effect for the barley which is not observed for the individual leaves of the dry grass spectrum included in the ASTERlib. According to the spectra obtained, it is difficult to draw a clear conclusion regarding to the performance of the NDVI and TES methods over senescent vegetation, since the NDVI classifies senescent vegetation as bare soil and the TES method classifies senescent vegetation as green vegetation (low MMD) in some cases.

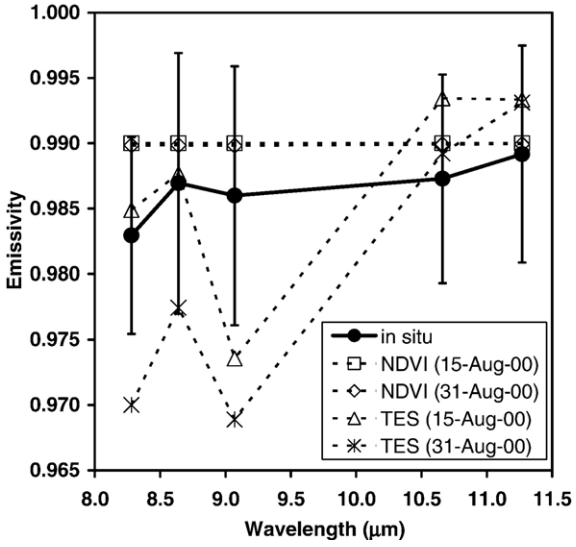

Fig. 10. Comparison between the emissivity spectrum obtained from field measurements over the corn plot (fully covered) and the emissivity spectra obtained with the NDVI and TES methods and extracted from ASTER images acquired on 15 and 31 August 2000. Error bars refer to the standard deviation of the mean value calculated from 40 field measurements.

3.5. Methods testing

Surface emissivities have been retrieved from ground-based measurements (Section 2.2) collected over corn (fully covered) and bare soil with the CIMEL instrument in 2004 and 2005. The measured values are assumed to be comparable to the emissivity spectra obtained in 2000 and 2001 from the ASTER images. Fig. 10 shows the emissivity spectrum measured in situ and the spectra obtained with the NDVI and TES methods for the corn

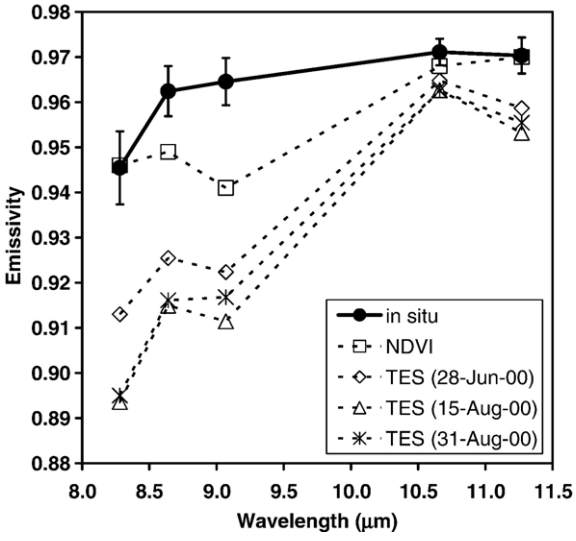

Fig. 11. Comparison between the emissivity spectrum obtained from field measurements over the bare soil and the emissivity spectra obtained with the NDVI and TES methods and extracted from ASTER images acquired on 28 June, 15 August and 31 August in 2000. Error bars refer to the standard deviation of the mean value calculated from 9 field measurements. The NDVI method provided the same emissivity spectra for the three different dates, so only one spectrum has been graphed.

Table 2
Comparison between the surface emissivities estimated with the NDVI and TES methods and the ones measured in situ over the corn (fully covered) and bare soil plots

Date	Plot	Method	Bias	σ	RMSE
15-Aug-00	Corn	NDVI	0.004	0.002	0.004
15-Aug-00	Corn	TES	0.000	0.007	0.007
31-Aug-00	Corn	NDVI	0.003	0.002	0.004
31-Aug-00	Corn	TES	−0.007	0.009	0.011
28-Jun-00	Bare soil	NDVI	−0.008	0.010	0.013
28-Jun-00	Bare soil	TES	−0.026	0.016	0.030
15-Aug-00	Bare soil	NDVI	−0.008	0.010	0.013
15-Aug-00	Bare soil	TES	−0.036	0.021	0.041
31-Aug-00	Bare soil	NDVI	−0.008	0.010	0.013
31-Aug-00	Bare soil	TES	−0.034	0.020	0.039

Bias refers to the mean difference between the values provided by the methods and the ones measured in situ for the five ASTER thermal bands, bias $= \frac{1}{5}\sum_{i=10}^{14}(\varepsilon_i^{\text{method}} - \varepsilon_i^{\text{in-situ}})$. σ refers to the standard deviation of the mean value given by the bias. The Root Mean Square Error (RMSE) is obtained as RMSE $= \sqrt{\text{bias}^2 + \sigma^2}$.

plot considered as fully vegetated (15-Aug-00 and 31-Aug-00). The spectrum measured in situ is a mean value obtained from the 40 measurements made over the corn. The spectra provided by the NDVI method falls within the mean and the standard deviation of the field measurements, whereas the TES method shows a significant deviation for bands 10 (~8.3 μm) and 12 (~9.1 μm). Moreover, the NDVI method provides almost the same spectrum for different dates, whereas the TES method provides different values in different dates. In a similar way, Fig. 11 shows the results obtained for the bare soil plot. In this case, 9 field measurements were made. The emissivity spectra obtained with the NDVI method is closer to the one measured in situ, despite that bands 11 (~8.6 μm) and 12 (~9.1 μm) do not fall within the mean and standard deviation values. Again, the NDVI method provides the same spectrum for different dates (for this reason only one soil spectrum obtained with the NDVI method has been graphed). The TES method provides different spectra at different dates, but in this case the differences are low.

In order to asses the accuracy of the methods, the mean difference between the values estimated with the method and the ones measured in situ for the five ASTER TIR bands (bias) and the standard deviation of the mean (σ) have been calculated. Then, the root mean square error (RMSE) has been obtained as RMSE $= \sqrt{\text{bias}^2 + \sigma^2}$. The values are shown in Table 2. The NDVI method provides accurate values for corn and bare soil plots, with RMSE < 0.005 and a RMSE < 0.015, respectively. The TES method provides also accurate values for the corn plot, with RSME ~ 0.01. However, the values provided over the bare soil plot are not accurate enough, with RMSE ranging between 0.03 and 0.04. Despite that field measurements over the alfalfa plot are not available, it is logical to assume that the emissivity spectrum would be similar to the corn, i.e., values spectrally constant and near to 0.99. Therefore, the emissivity spectra obtained with the NDVI method over the alfalfa plot (see Fig. 5) is more in accordance with field measurements that the ones provided by the TES method. Due to the problems involved in the emissivity estimation over senescent vegetation areas, it is difficult to show a reliable test over these kinds of plots. Field measurements over non-irrigated wheat and dry shrubs has shown a decrease on emissivity with increasing wavelength (not shown in this paper), also observed in the dry grass (see Fig. 9), which confirms that NDVI and TES methods do not provides good results for senescent vegetation.

3.6. Discrimination of different crops using NDVI and MMD values

Distinguishing among green vegetation, senescent vegetation, and bare soil is important because ground cover strongly

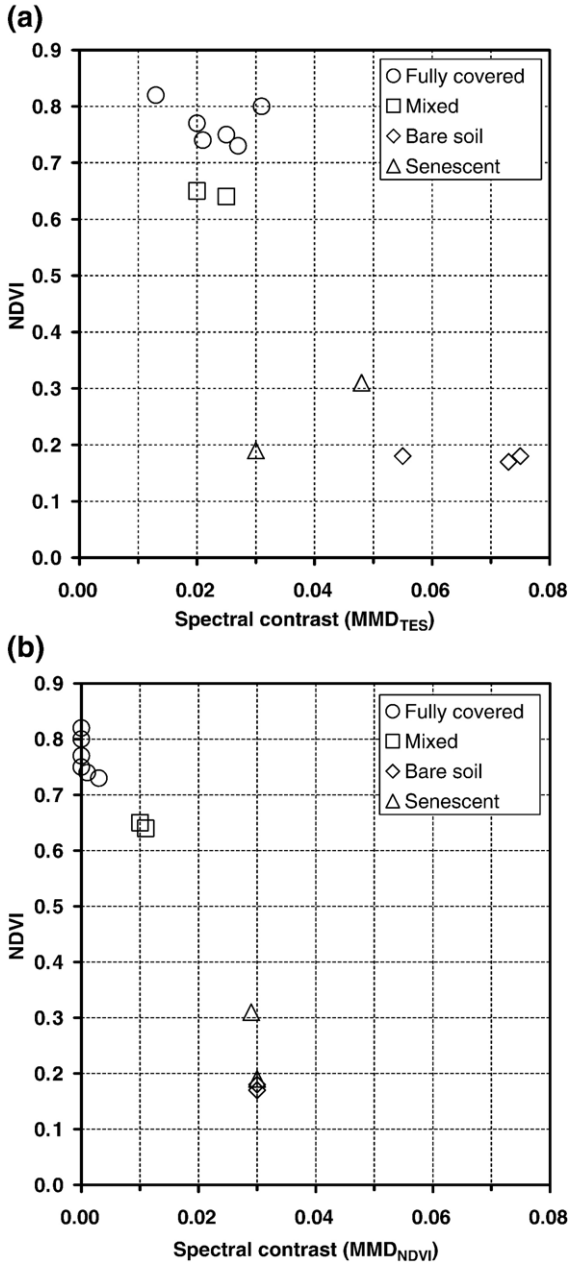

Fig. 12. Plot of NDVI vs. MMD for different crops (alfalfa, bare soil, irrigated corn and non-irrigated barley) corresponding to the five ASTER images acquired in 2000 and 2001. MMD values have been obtained from Eq. (4) using emissivity values recovered with a) TES algorithm (MMD_{TES}) and b) NDVI method (MMD_{NDVI}).

influences the surface thermal gradient, surface roughness and surface heat flux. For this purpose, French et al. (2000) suggest using the spectral emissivity contrast or MMD combined with a vegetation index such as NDVI to distinguish these surface types. Green and senescent vegetation both have similar MMD values, but different NDVI values; senescent vegetation and bare soil have similar NDVI values but different MMD values; and green vegetation and soil have different NDVI values and, generally, different MMD values. Thus, when NDVI values only are used, it is difficult to distinguish between senescent vegetation and bare soil, and when MMD values only are used, it is difficult to distinguish between green and senescent vegetation.

Fig. 12 shows the plot of NDVI versus MMD values obtained from Eq. (4). MMD values have been obtained from the emissivities estimated with the TES (Fig. 12a) and NDVI (Fig. 12b) methods. Green vegetation over fully covered or mixed plots is well distinguished in both cases. Bare soil and senescent vegetation are well distinguished from the MMD values obtained with the TES method (Fig. 12a), but not from MMD values obtained with the NDVI method (Fig. 12b). In fact, the NDVI method always provides a MMD <0.03, because the soil spectrum used in the method has a low spectral contrast and non-irrigated barely is classified as a soil ($NDVI<NDVI_s$). According to the results obtained with the TES method, the following thresholds could be considered in order to distinguish between different crops:

i) fully covered area, $NDV>0.7$ and $MMD<0.03$,
ii) mixed area, $0.2\leq NDV\leq 0.7$ and $MMD<0.03$,
iii) senescent vegetation, $0.7\geq NDVI\geq 0.2$ and $0.3\leq MMD\leq 0.5$,
iv) bare soil, $NDVI<0.2$ and $MMD>0.5$.

In this way, VNIR and TIR data could be combined in order to classify the different pixels as green vegetation, senescent vegetation and bare soil, and then using emissivity values estimated from NDVI values when the TES fails, or vice versa, although it is well to remember that the thresholds for the NDVI and MMD have been obtained for the study area, so our findings may not be representative of all cases. Moreover, an additional solution is needed for senescent vegetation, in which NDVI and TES methods do not provide satisfactory results.

4. Summary and conclusions

In this paper two different methods have been applied to high spatial resolution and multispectral thermal data in order to retrieve land surface emissivity over an agricultural area: the NDVI method, which uses visible and near infrared data, and the TES method, which uses thermal infrared data. A comparison between them over different plots (alfalfa, soil, corn and barley) and using ASTER images acquired in different dates shows similar values for ASTER bands 13 and 14, with differences typically lower than 0.6% and 1.5%, respectively. The NDVI and TES methods have been also compared to laboratory spectra and surface emissivities measured in situ. The NDVI method shows in general a better shape for the emissivity spectra than the TES method, with values also closer to the ones measured in situ. RMSE values lower than 0.005 for fully vegetated areas and lower than 0.015 for bare soil have been obtained with the NDVI method. The TES method provided a RMSE ~ 0.01 over fully vegetated areas, but errors higher than 0.03 for bare soil. ASTER bands 12 and 13 located in the spectral region 10–12 μm provided the best results, which can be due to the low atmospheric absorption and the low variation on the emissivity values in comparison with the other bands, located in the spectral region 8–9.5 μm. It should be noted that surface emissivities can be also retrieved using only the NEM module, which also provides good results, as has been pointed by Sobrino et al. (2002b) and Jiménez-Muñoz et al. (2003).

Different advantages and disadvantages can be found when comparing the NDVI and TES methods. Hence, the TES method provides accurate results for surface emissivities, in general within 0.015, overall for rocks surfaces. However, the accuracy of the TES is expected to decrease for surfaces with low MMD values, as is the case of agricultural areas. In this case, the NDVI method is expected to provide slightly better results. However, the NDVI method is not applicable over rocks surfaces, and also surfaces with negative NDVI values, as water, snow and ice, despite these surfaces have well-known emissivity spectra. The performance of the TES method over surfaces with low MMD values needs more analysis and validation, as well as the adaptation of the NDVI method to rocks surfaces. One advantage for the TES method is the capability of recovering land surface temperature jointly with surface emissivities, whereas the NDVI method only retrieves land surface emissivity. Predicting surface emissivities from visible and near-infrared data provides two main advantages to the NDVI method: i) sensors onboard satellites provide a higher spatial resolution for visible and near infrared than thermal infrared bands, so higher spatial resolution emissivity maps can be obtained (in the case of ASTER, emissivity maps with a spatial resolution of 15 m can be obtained when the NDVI method is used, in comparison with the spatial resolution of 90 m obtained with the TES method), and ii) the NDVI method can be applied even to sensors with only one thermal band, provided that these sensors have red and near infrared bands, whereas TES method needs at least four thermal bands.

It should be noted that in general cases a cavity term should be added to the NDVI method (Sobrino & Raissouni, 2000; Valor & Caselles, 1996), but some geometrical factors are needed in order to calculate this term. If a priori knowledge of the site is not available, a mean value for the geometrical factors involved in the cavity term could be chosen. Over agricultural areas with high emissivity values for the soils the cavity term could be neglected, overall for surfaces with a high proportion of vegetation. However, when the geometrical factors for the crop are measured in situ, the cavity term can be particularized and more accurate values will be expected with the NDVI method. There is another point that should be taken into account when analyzing the NDVI methodology, which refers to the estimation of the proportion of vegetation or vegetation fraction cover from NDVI values (Eq. (6)), according to Carlson and Ripley (1997). This is a simple way of estimation proportion of

vegetation and accurate enough in order to apply the NDVI method. However, a multispectral analysis by endmembers could lead to an improvement on the proportion of vegetation estimation, despite that the main error source in the NDVI methodology is the selection of the soil emissivity.

TES scales emissivity data with low and high MMD values differently. Under some circumstances, it appears that threshold test fails, causing "jumps" or step discontinuities especially in the emissivity product. In our images of Barrax, the high standard deviation values obtained with the TES method for the boxes of 3×3 pixels selected in order to extract the results from the ASTER images do suggest that inappropriate scaling did occur in some cases. This misclassification leads to the most serious failures of TES that we have encountered. The success of the NDVI method, at least for the plots considered in this study, suggests that the ASTER Standard Product could be modified to incorporate aspects of the NDVI approach, with the goal of minimizing the "jumps" at least for daytime data. In Sobrino et al. (2002b) a combination of methods was proposed depending on NDVI values. In this paper, the plot of NDVI versus MMD has been used in order to discriminate different crops. Particular NDVI and MMD thresholds have been proposed to classify the pixels into bare soil, green grass and senescent vegetation. In this way, the TIR data could be complemented with the VNIR data in order to apply the NDVI method over surfaces in which the TES method fails. Emissivity retrieval over senescent vegetation needs further research, since the NDVI and the TES methods do not classify these pixels properly.

Acknowledgements

We thank to the European Union (EAGLE, project SST3-CT-2003-502057), the Ministerio de Ciencia y Tecnología (DATASAT, project ESP2005-07724-C05-04) and the European Space Agency (SPARC, project RFQ/3-10824/03/NL/FF) for the financial support. The University of Washington participation was supported by NASA's ASTER project. We thank Cindy Grove, JPL, for laboratory measurements of soil spectra. The comments of four anonymous reviewers greatly improved the mansucript.

References

Abrams, M. (2000). The advanced Spaceborne Thermal Emission and Reflection Radiometer (ASTER): Data products for the high spatial resolution imager on NASA's Terra platform. *International Journal of Remote Sensing*, *21*(5), 847−859.

Abreu, L. W., & Anderson, G. P. (Eds.) (1996). *The MODTRAN 2/3 report and LOWTRAN 7 MODEL, Modtran report, contract F19628-91-C-0132*: Philips Laboratory.

Becker, F., & Li, Z. -L. (1990). Temperature independent spectral indices in thermal infrared bands. *Remote Sensing of Environment*, *32*, 17−33.

Becker, F., & Li, Z. -L. (1995). Surface temperature and emissivity at various scales: Definition, measurement and related problems. *Remote Sensing Review*, *12*, 225−253.

Carlson, T. N., & Ripley, D. A. (1997). On the relation between NDVI, fractional vegetation cover, and leaf area index. *Remote Sensing of Environment*, *62*, 241−252.

Dash, P., Göttsche, F. -M., Olesen, F. -S., & Fischer, H. (2002). Land surface temperature and emissivity estimation from passive sensor data: Theory and practice-current trends. *International Journal of Remote Sensing*, *23*(13), 2563−2594.

French, A. N., Schmugge, T. J., & Kustas, W. P. (2000). Discrimination of senescent vegetation using thermal emissivity contrast. *Remote Sensing of Environment*, *74*, 249−254.

Gillespie, A. R. (1985). Lithologic mapping of silicate rocks using TIMS. *The TIMS data users' workshop, JPL Publication, Vol. 86–38* (pp. 29–44).

Gillespie, A. R., Rokugawa, S., Hook, S., Matsunaga, T., & Kahle, A. B. (1998). A temperature and emissivity separation algorithm for Advanced Spaceborne Thermal Emission and Reflection Radiometer (ASTER) images. *IEEE Transactions on Geoscience and Remote Sensing*, *36*, 1113−1126.

Goïta, K., & Royer, A. (1997). Surface temperature and emissivity separability over land surface from combined TIR and SWIR AVHRR data. *IEEE Transactions on Geoscience and Remote Sensing*, *35*(3), 718−733.

Herman, B. M., & Browing, S. R. (1965). A numerical solution to the equation of radiative transfer. *Journal of Atmospheric Science*, *22*, 559−566.

Jiménez-Muñoz, J. C., Sobrino, J. A., Gillespie, A., & Sabol, D. (2003). Separación emisividad/temperatura a partir de datos DAIS y aplicación del contraste espectral para discriminar distintos tipos de vegetación. *Revista de Teledetección*, *19*, 51−58.

Jiménez-Muñoz, J.C., Sobrino, J.A., Guanter, L., Moreno, J., Plaza, A., & Martínez, P. (submitted for publication). Land surface emissivity retrieval based on FVC estimations from PROBA/CHRIS VNIR data, Agricultural and Forest Meteorology.

Kahle, A. B., Madura, D. P., & Soha, J. M. (1980). Middle infrared multispectral aircraft scanner data: Analysis for geological applications. *Applied Optics*, *19*(14), 2279−2290.

Kealy, P. S., & Hook, S. (1993). Separating temperature and emissivity in thermal infrared multispectral scanner data: Implication for recovering land surface temperatures. *IEEE Transactions on Geoscience and Remote Sensing*, *31*, 1155−1164.

Lyon, R. J. P. (1965). Analysis of rocks by spectral infrared emission (8 to 25 microns). *Economic Geology*, *60*, 715−736.

Moreno, J., Calera, A., Caselles, V., Cisneros, J. M., Martínez-Lozano, J. A., Meliá, J., et al. (2001). The measurement programme at Barrax. *DAISEX final results workshop, Noordwijk (Holland), SP-499* (pp. 43−51).

Palluconi, F., Hoover, G., Alley, R., Jentoft-Nilsen, M., & Thompson, T. (1999). *An atmospheric correction method for ASTER thermal radiometry over land.Algorithm Theoretical Basis Document* Pasadena, CA: Jet Propulsion Laboratory. Available on-line at http://www.science.aster.ersdac.or.jp/en/documnts/pdf/2b01t.pdf

Payan, V., & Royer, A. (2004). Analysis of Temperature and Emissivity Separation (TES) algorithm applicability and sensitivity. *International Journal of Remote Sensing*, *25*(1), 15−37.

Slater, P. N., Biggar, S. F., Holm, R. G., Jackson, R. D., Mao, Y., Moran, M. S., et al. (1987). Reflectance- and radiance-based methods for the in-flight absolute calibration of multispectral sensors. *Remote Sensing of Environment*, *22*, 11−37.

Sobrino, J. A., Caselles, V., & Becker, F. (1990). Significance of the remotely sensed thermal infrared measurements obtained over a citrus orchard. *ISPRS Photogrammetric Engineering and Remote Sensing*, *44*, 343−354.

Sobrino, J. A., & Raissouni, N. (2000). Toward remote sensing methods for land cover dynamic monitoring. Application to Morocco. *International Journal of Remote Sensing*, *21*, 353−366.

Sobrino, J. A., Li, Z. -L., Soria, G., & Jiménez, J. C. (2002). Land surface temperature and emissivity retrieval from remote sensing data. *Recent Research Developments in Geophysics*, *4*, 21−44.

Sobrino, J. A., Jiménez-Muñoz, J. C., Labed-Nachbrand, J., & Nerry, F. (2002). Surface emissivity retrieval from Digital Airborne Imaging Spectrometer data. *Journal of Geophysical Research*, *107*(D23), 4729, doi:10.1029/2002JD002197.

Thome, K., Biggar, S., & Takashima, T. (1999). *ASTER Level 2B1 — Surface radiance and ASTER Level 2B5 — Surface reflectance.Algorithm Theoretical Basis Document* Tucson, Arizona: Optical Sciences Center, University of Arizona. Availabe on-line at http://www.science.aster.ersdac.or.jp/en/documnts/pdf/2b0105.pdf

Valor, E., & Caselles, V. (1996). Mapping land surface emissivity from NDVI: Application to European, African and South American areas. *Remote Sensing of Environment*, *57*, 167−184.

Van de Griend, A. A., & Owe, M. (1993). On the relationship between thermal emissivity and the normalized difference vegetation index for natural surfaces. *International Journal of Remote Sensing*, *14*(6), 1119−1131.

Watson, K. (1992). Two-temperature method for measuring emissivity. *Remote Sensing of Environment*, *42*, 117−121.